Proliferation index and pseudoprogression as predictors of the therapeutic efficacy of suicide gene therapy for canine melanoma

Chiara Fondello*, Lucrecia Agnetti*, Gerardo C. Glikin and Liliana M.E. Finocchiaro

In our veterinary clinical trials, the combination of systemic immunotherapy with local herpes simplex virus thymidine kinase/ganciclovir suicide gene (SG) treatment induced tumor pseudoprogression as part of a strong local antitumor response. This phenomenon could be owing to tumor inflammation, increased vascular permeability and to different tumor growth rates before, during and after SG therapy. The proliferation index (PI: the fraction of viable cells in S, G2/M, and hyperdiploid phases) would reflect the in-vivo and in-vitro proportion of proliferating melanoma cells in the absence of treatment (PI_B) or in response to SG (PI_{SG}). The extent of in-vivo and in-vitro melanoma cells responses to SG exhibited a reverse correlation with PI_B and a direct correlation with PI_{SG}. Then, the final SG outcome depended on the balance between PI_B-dependent 'regrowth resistance' versus 'regrowth sensitivity' to SG treatment. In all the cell lines derived from canine tumors presenting partial responses to SG treatment, PI_{SG} prevailed over PI_B. Conversely, as more aggressive was the tumor (greater PI_B of the cell line), the more the balance displacement towards 'regrowth resistance' over SG 'regrowth sensitivity'. All these parameters could have a prognostic value for SG treatment response and provide a glimpse at the clinical benefit of this therapy. ***Melanoma Res*** **00:000–000**

Melanoma Research 2018, **00**:000–000

Keywords: canine melanoma, herpes simplex virus thymidine kinase, proliferation index, pseudoprogression, suicide gene

Gene Transfer Unit, Institute of Oncology Angel H. Roffo, University of Buenos Aires, Buenos Aires, Argentina

Correspondence to Liliana M.E. Finocchiaro, PhD, Unidad de Transferencia Genética, Instituto de Oncología Ángel H. Roffo, Universidad de Buenos Aires, Av. San Martín 5481, 1417 Buenos Aires, Argentina
Tel: +54 115 287 5300; e-mail: finolili@hotmail.com

*Chiara Fondello and Lucrecia Agnetti contributed equally to the writing of this article.

Received 11 August 2018 **Accepted** 7 December 2018

Introduction

Canine malignant melanoma is an extremely aggressive form of cancer clinically similar to human melanoma [1,2]. Both human and canine malignant melanomas tend to metastasize early in the disease process and are often fatal [3,4]. Significant negative prognostic factors comprise size, occurrence of metastasis, stage, diverse histological criteria and excision of the tumor burden with narrow or no margins [5–7].

Immuno-oncology has emerged as an exciting new approach to melanoma treatment [8–14]. An increasing number of studies have shown high heterogeneity of responses in patients receiving immunotherapy [15,16]. Some patients experience an initial tumor growth followed by reduction in total tumor burden. Such atypical immune-related responses termed pseudoprogression (PP) pose growing clinical challenges [15,16]. Traditional response standards applied at the time of initial increase in tumor burden can falsely designate this as treatment failure leading to inappropriate termination of therapy [15,16].

Most of the veterinary cancer gene therapy trials on patients with spontaneous tumors could be classified as immunogenic therapy and were performed with nonviral vectors [17,18]. PP response patterns were identified in our veterinary clinical trials, implementing a combination of systemic gene immunotherapy and intratumor suicide gene (SG) therapy. In these trials, intratumor SG therapy with thymidine kinase from the herpes simplex virus thymidine kinase (HSV*tk*), codelivered with the prodrug ganciclovir (GCV), induced a strong local antitumor response [8–11,17,18].

Although PP is becoming increasingly recognized by immunologists, the mechanisms and biological significance of this phenomenon remain enigmatic. The wide intratumoral heterogeneity and molecular complexity of melanoma tumors suggests that the clinical diversity of the disease arise from highly plastic subpopulations of dormant and proliferating melanomas cells [19–21]. Understanding key cellular processes, such as cell cycle regulation and cell death, is essential for better diagnosis, accurate assessment of prognosis and rational design of effective therapeutics. Biological markers that correlate with the clinical course of this disease could have a prognostic value for treatment efficacy [22,23].

In previous reports [24,25] we demonstrated that melanoma cell lines derived from tumors of feline and canine veterinary

0960-8931 DOI: 10.1097/CMR.0000000000000567

patients reestablished the morphology, physiology and cell heterogeneity of their respective parental tumors. In this context, we explored the potential of PP and increased proliferation index (PI) in response to SG therapy as biological indicators of both in-vivo and in-vitro effectiveness of this therapeutic agent.

Materials and methods

Veterinary patients and treatment

Dogs with a confirmed histopathological diagnostic of melanoma were recruited for a study as it was reported [8–11]. Their owners were notified about the experimental nature of the treatment, and all of them granted written informed consent for treatment [8–11]. All the procedures related to the treatment were performed by qualified attending veterinary professionals, following the laws and regulations of our country (Argentina). All scientific and ethical issues related to the veterinary clinical trial were evaluated and approved by the corresponding committee of the granting agency (ANPCYT, Argentina). These spontaneous melanoma canine patients received twice a week during 5 weeks, intratumor and peritumor injection at multiple sites of lipid-complexed plasmid DNA encoding HSV*tk* (1–4 mg DNA codelivered with 5–20 mg GCV according the tumor size). After 24 and 48 h following SG plus GCV delivery, patients orally took 400–800 mg of acyclovir according to their weight. They continued with a weekly local treatment chronically or until disappearance of any evidence of local disease [8]. In addition, patients were clinically controlled and treated once a week for 5 weeks with a subcutaneous vaccine composed of autologous and/or allogeneic formolized tumor cells and irradiated living CHO xenogeneic cells producing 20–30 mg of hIL-2 and hGM-CSF [9]. To check the possible metastatic spread of the disease, thoracic radiographs and abdominal echographs were done before treatment and every month during the first 6 months under treatment and, at longer intervals up to 6 months in long-term surviving patients as previously described [8]. As superficial tumors often display irregular shapes, three different sets of caliper measurements were performed for each mass, and the volume was expressed as the mean ± SEM. Tumor volumes were calculated as: $4/3 \times \pi \times r_1 \times r_2 \times r_3$ [8].

Establishment of cell cultures from canine melanoma patients

Primary cell lines derived from surgically excised lymph nodes metastasis (*Btl*) or from oral (*Ay*, *Bk*, *Bl*, *Br*, *Bt*, *Btl*, *Cl*, *Ds*, *Fk*, *Lo*, *Ov*, *Rk*, *Rka*, *Sc*, and *Tr*), nasal (*Ch*) and ocular (*Rd*) canine melanomas were obtained by enzymatic digestion of tumor fragments with 0.01% Pronase (Sigma, St Louis, Missouri, USA) and 0.035% DNase (Sigma) or by mechanical disruption in serum-free culture medium [25]. They were cultured as monolayers and multicellular spheroids at 37°C in a humidified atmosphere of 95% air and 5% CO_2 with DMEM/F12 medium (Invitrogen, Carlsbad, California, USA) containing 10% fetal bovine serum (Invitrogen), 10 mmol/l HEPES (pH 7.4), and antibiotics [25]. Serial passages were done by trypsinization (0.25% trypsin and 0.02% EDTA in PBS) of subconfluent monolayers [25].

Plasmids

Plasmid psCMV*tk* (4.5 kbp) carries an Eco RI/Bgl II fragment (1.2 kbp) containing HSV*tk* gene, cloned in the sites Eco RI/BamH1 of psCMV (3.3 kbp) downstream of the CMV promoter and upstream of poly A sequences, and the kanamycin resistance gene for selection in *Escherichia coli* [25]. psCMV*β* was built by replacing the HSV thymidine kinase gene of psCMV*tk* by *E. coli* β-galactosidase gene from pCMVβ [25]. Plasmids were amplified in *E. coli* DH5α (Invitrogen), grown in LB medium containing 100 μg/ml neomycin and purified by ion-exchange chromatography (Qiagen, Valencia, California, USA).

Liposome preparation and in-vitro lipofection

DC-Chol (3β[*N*-(*N*′,*N*′-dimethylaminoethane)-carbamoyl cholesterol]) and DMRIE (1,2-dimyristyloxypropyl-3-dimethyl-hydroxyethilammonium bromide) were synthesized and kindly provided by Dr Eduardo M. Rustoy (Department of Organic Chemistry, Faculty of Exact and Natural Sciences, University of Buenos Aires, Buenos Aires, Argentina). DOPE (1,2-dioleoyl-*sn*-glycero-3-phosphatidyl ethanolamine) was purchased from Sigma (St Louis, Missouri, USA). Liposomes were prepared at lipid/colipid molar ratios of 3 : 2 (DC-Chol : DOPE) or 1 : 1 (DMRIE : DOPE) by sonication as described [25]. Optimal lipid mixtures were determined for every cell line [24,25]. Cultured cells at a density of 5×10^4 cells/cm^2 (about 40% confluence) were exposed to lipoplexes (1 μl liposomes/cm^2 and 0.5 μg DNA/cm^2) during 4–6 h [24,25].

β-galactosidase staining

To measure gene transfer efficiency, psCMVβ lipofected cells were trypsinized, fixed in suspension, stained with 5-bromo-4-chloro-3-indolyl β-D-galactopyranoside (X-GAL; Sigma, St Louis, Missouri, USA) and counted using an inverted phase contrast microscope [24,25].

Sensitivity to ganciclovir assay

Twenty-four hours after lipofection, transiently HSV*tk*- or βgal-expressing cells were reseeded on regular plates as monolayers ($4–7 \times 10^3$ cells) or at 2.5, 5, 10 and 20×10^4 cells/ml over agar coverage as spheroids and incubated with medium containing 5 μg/ml GCV (Richet, Buenos Aires, Argentina). After 5 days in monolayers or 12 days in spheroids, cell survival was quantified using the acid phosphatase assay [25]. In brief, spheroids growing in liquid overlay were transferred to 96-well microplates, washed and finally incubated for 90 min at 37°C, with 100 μl per well of the assay buffer (0.1 mol/l sodium acetate, 0.1% Triton-X-100, supplemented with *p*-nitrophenyl phosphate). Following incubation, 10 μl of 1 N NaOH was supplemented to each well, and absorption at 405 nm was measured within 10 min.

Flow cytometry cell cycle analysis

Untreated cells or HSV*tk*-expressing, or *βgal*-expressing cells, cultured in the presence of 1 μg/ml GCV for 48 h, were trypsinized, fixed in 70% (v/v) ethanol at − 20°C for 1 h, treated with RNase, stained with 10 μg/ml propidium iodide for 30 min, and subjected to single-channel flow cytometry on a Becton Dickinson FACScan (Franklin Lakes, New Jersey, USA), with collection and analysis of data performed using Becton Dickinson CELLQuest software (BD Biosciences, San Jose, California, USA) [24].

Statistical analysis

Results were expressed as mean ± SEM (*n*: number of experiments corresponding to independent assays). Differences between groups were analyzed using unpaired Student's *t*-test (if two groups), one-way analysis of variance followed by Tukey's test (if more than two groups), or two-way analysis of variance followed by Bonferroni's test (if two nominal variables). Correlations were determined by Pearson's test with GraphPad Prism program (GraphPad Software Inc., San Diego, California, USA). *P* values less than 0.05 values were considered statistically significant.

Results and discussion

In-vivo suicide gene treatment displayed a significant rate of tumor pseudoprogression

In our veterinary clinical trials, the combination of systemic immunotherapy with local HSV*tk*/GCV SG therapy provoked several atypical patterns of tumor response. Fluctuations in tumor volume were recorded: at times mimicking tumor progression and at times tumor reduction (Fig. 1). This paradoxical transient increase of tumor size (PP) attributable to SG treatment effects rather than early tumor progression finally resolved in tumor shrinking or stabilization.

As shown in Fig. 1, among the 17 tumors studied, nine presented in-vivo PP (*Ay*, *Bk*, *Cl*, *Ds*, *Ov*, *Rk*, *Rka*, *Sc*, and *Tr*). Six (*Ay*, *Cl*, *Ov*, *Rk*, *Rka*, and *Tr*) of these nine PP tumors concluded in partial responses (PR, tumor size reduction > 50%) and three (*Ds*, *Bk*, and *Sc*) in stable disease (SD, tumor size increase or decrease <50%). To

Fig. 1

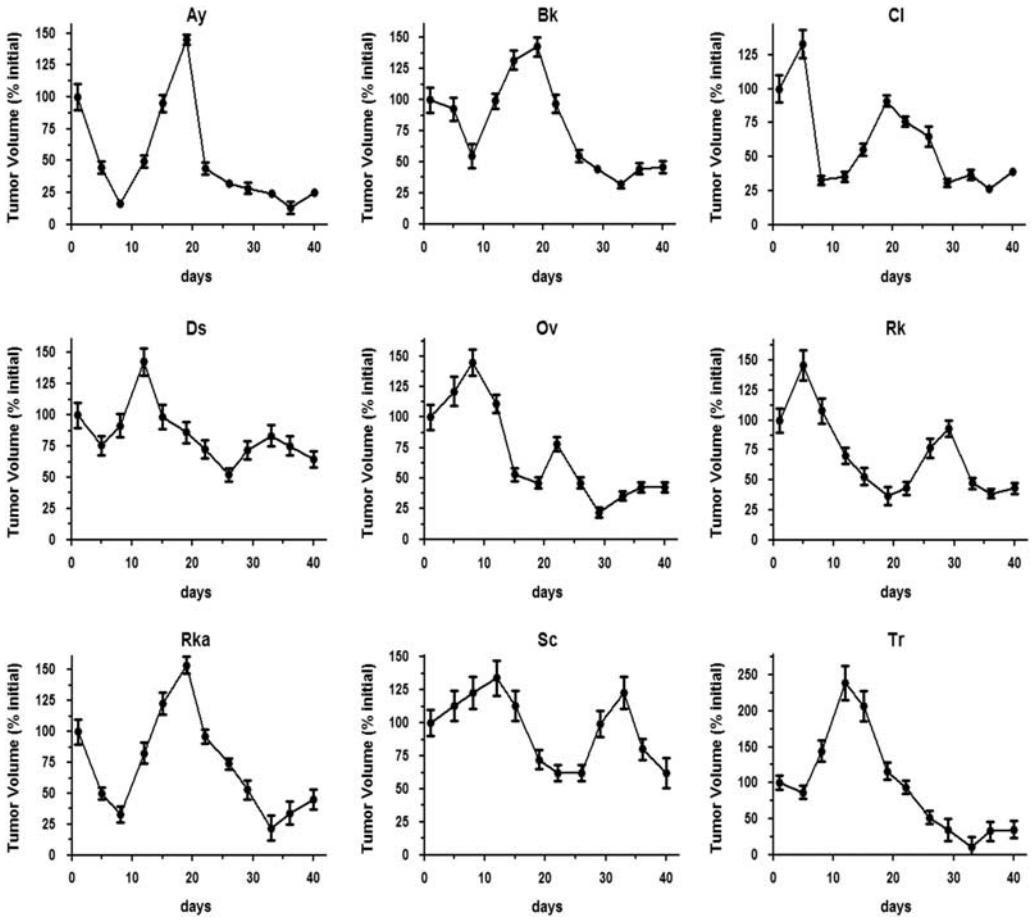

In-vivo individual tumor responses that displayed pseudoprogression during 40 days under suicide gene system (herpes simplex virus thymidine kinase/ganciclovir) treatment. Each value was relative to the respective initial tumor volume. Canine patients were treated and tumor measurements were performed as described in the Materials and methods section.

Fig. 2

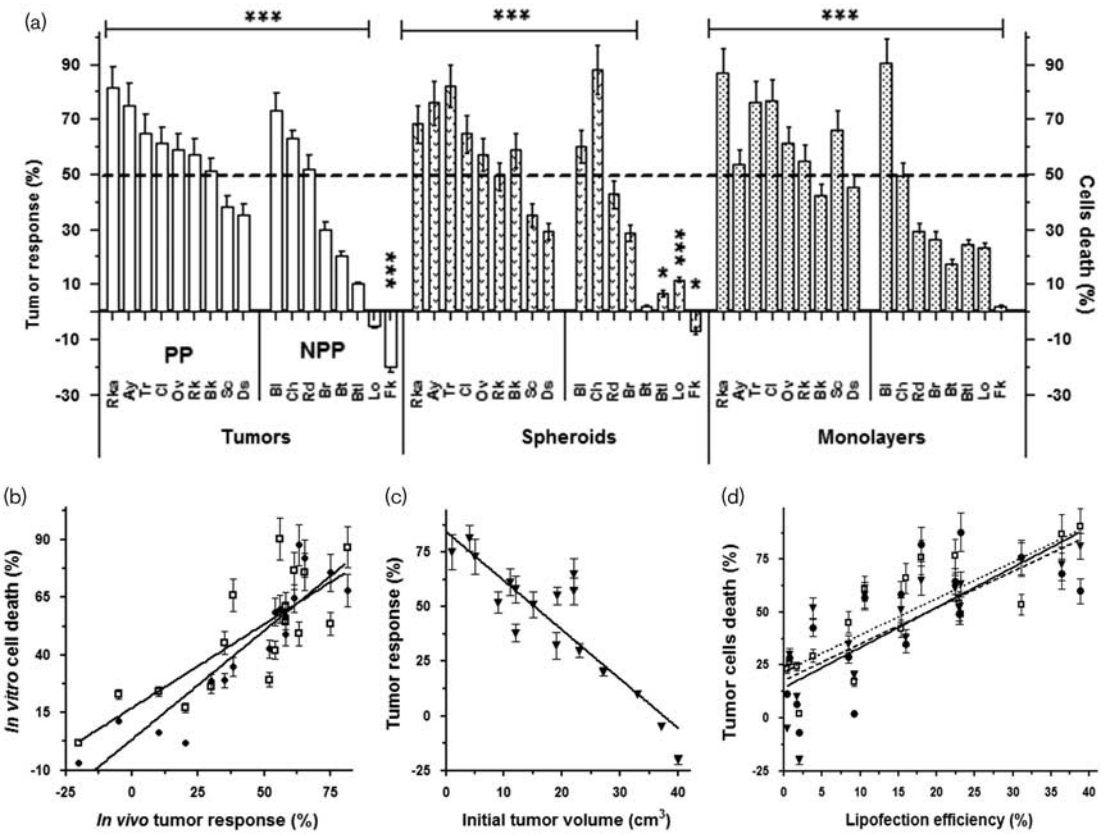

Response to SG *vs*	*In vivo* tumors		Spheroids		Monolayers	
	R^2	*P*<	R^2	*P*<	R^2	*P*<
Lipofection efficiency (%)	0.674	0.0001	0.540	0.0005	0.690	0.0001
Final tumor response (%)	-	-	0.847	0.0001	0.635	0.0001
Initial tumor volume (%)	0.805	0.0001	-	-	-	-

Sensitivity to SG system of in-vivo tumors, and their respective spheroids and monolayers (a). Being V_i and V_f respectively the initial (day 0) and final in-vivo tumor (day 40) volumes, the tumor response was defined as follows: $TR = (V_i - V_f)/V_i \times 100$. Tumor volumes were determined as described in Materials and methods section. The cell death values for spheroids and monolayers were analogously derived from tumor cells survival (*S*) data obtained by the acid phosphatase assay as described in the Materials and methods section: $CD = (S_i - S_f)/S_i \times 100$. These results represent the mean ± SEM of $n \geq 4$ independent experiments. *Versus its respective *βgal* expressing monolayers or spheroids, or final versus initial tumor volume. $^*P < 0.05$, $^{**}P < 0.01$, $^{***}P < 0.001$. (b) Correlation between the in-vivo tumor responses to SG and that of their respective monolayers and spheroids. (c) Correlation between the initial size of the in-vivo tumors and their response to SG system. (d) Correlation between in-vitro lipofection efficiency and SG sensitivity of monolayers (□), spheroids (●) and in-vivo tumors (▼). Statistical values were determined by the Pearson test with the GraphPad program. NPP, nonpseudoprogression; PP, pseudoprogression; SG, suicide gene.

avoid favorably biased conclusions, the negative value of SEM was deducted for assignment to PR group.

The in-vivo tumor sensitivity to the suicide gene was reflected by their respective derived cell lines

As already demonstrated in previous work [24,25], canine melanoma cell lines reflected the SG sensitivity of their respective tumors (Fig. 2). Regardless of the presence of PP, the pattern of in-vivo tumor responses of these veterinary patients was similar to the in-vitro cellular responses to SG, especially those of tumor-derived spheroids (Fig. 2a). This issue was reinforced by the high correlation in SG sensitivity between the in-vivo tumor and their respective derived cell lines in both spatial configurations (Fig. 2b).

In contrast, as suggested by the significant correlation ($P < 0.0001$) exhibited in Fig. 2c, the initial size of the in-vivo tumors determined their response to the SG system, being higher in patients with smaller tumors.

All tumors presenting in-vivo PR (*Rka*, *Ay*, *Tr*, *Cl*, *Ov*, *Rk*, *Bl*, and *Ch*) resulted in cell lines highly sensitive to SG lipofection in both spatial configurations. Of nine tumors exhibiting SD (*Bk*, *Sc*, *Ds*, *Rd*, *Br*, *Bt*, *Btl*, *Lo*, and *Fk*), eight of them as monolayers, and seven as spheroids, were sensitive to the SG system. *Fk* cell line, arising from

Table 1 Effects of suicide gene (herpes simplex virus thymidine kinase/ganciclovir) on the in-vitro and in-vivo responses and proliferation index of canine melanoma cells

	Response to suicide gene system (%)							
		In vitro		PI (%)				PI_B vs. PI_{SG}
Tumor/cell lines	In-vivo tumors	Mnl	Sph	In-vitro lipofection rate (%)	PI_B	PI_{SG}	PI_{SG-B}	*P*
PP tumors								
Rka	81.3±8 (PR)	90.5±9	60.0±6	38.8±8.9	37.1±2.1	76.4±5.1	39.3	<0.001
Ay	75.0±8 (PR)	53.6±5	75.9±8	31.1±8.1	40.6±2.2	64.7±3.8	24.1	<0.002
Tr	65.0±7 (PR)	76.0±8	82.0±8	18.0±2.9	38.6±2.3	70.7±6.1	32.1	<0.002
Cl	61.3±1 (PR)	76.6±8	64.6±7	22.4±6.8	40.1±2.1	76.8±5	36.7	<0.01
Ov	58.8±5 (PR)	61.1±6	57.0±5	10.6±3.0	33.7±1.7	66.8±3.6	33.1	<0.02
Rk	57.1±6 (PR)	54.6±5	49.1±5	23.0±6.5	39.1±3.4	74.2±3–7	35.1	<0.005
Bk	51.0±5 (SD)	42.1±3	58.6±6	15.3±6.9	44.1±3.3	68.6±3.6	24.5	<0.01
Sc	38.0±4 (SD)	65.5±7	34.8±3	16.0±2.3	45.6±2.2	63.5±2.8	17.9	<0.05
Ds	35.1±2 (SD)	45.2±6	29.1±3	8.5±4,2	41.2±2.3	61.2±3.6	20.0	<0.05
NPP tumors								
Bl	72.9±8 (PR)	86.8±9	68.1±7	36.4±8.6	44.5±2.4	69.5±3.7	25.0	<0.02
Ch	63.2±6 (PR)	49.3±6	87.8±9	23.2±7.5	47.3±2,8	70.7±4.1	23.4	<0.02
Rd	52.1±5 (SD)	29.3±2	42.7±4	3.8±0.1	45.0±2.7	55.6±2.9	10.6	NS
Br	30.0±3 (SD)	26.2±3	28.6±3	0.7±0.2	45.8±4.1	58.8±4.5	13.0	NS
Bt	20.2±2 (SD)	17.2±2	2.0±0.2	9.2±3.4	49.0±2.4	45.8±2.4	−3.2	NS
Btl	10.2±1 (SD)	24.3±2	6.6±0.7	1.7±0.6	50.3±2.5	58.9±2.5	8.6	NS
Lo	−5.0±1 (SD)	23.1±2	11.5±1	0.4±0.2	57.5±3.2	52.6±3.5	−4.9	NS
Fk	−20.1±2 (SD)	1.6±0.1	−7.3±0.7	2.0±0.3	55.6±2.6	43.0±2.4	−12.6	NS

The results represent the mean±SEM of $n \geq 4$ independent experiments.
PI was determined by evaluating the percentage of viable cells in the S, G_2/M, and hyperdiploid phases as described in the Materials and methods section.
Response to suicide gene system (%): from the graphics displayed in Fig. 2a.
Mnl, monolayers; NPP, nonpseudoprogression; PI, proliferation index; PI_B, PI of untreated control cells; PI_{SG}, PI of suicide gene-expressing cells; PI_{SG-B}, net PI increase due to suicide gene treatment obtained by subtracting PI_B of the respective PI_{SG}; PP, pseudoprogression; PR, partial response; SD, stable disease; Sph, spheroids.
P values were calculated by two-tailed unpaired *t*-test.

highly proliferative advanced tumor, was not sensitive to the SG system in any culture configuration.

A very encouraging outcome was that of *Br* cell line, where less than 1% of SG-expressing cells were enough to destroy 26, 29, and 30% of monolayers, spheroids, and in-vivo tumor cells, respectively (Fig. 2a).

As observed in Fig. 2d, a direct correlation was found between in-vivo and in-vitro canine melanoma cells response to the SG in both spatial configurations and their respective lipofection efficiencies ($P < 0.001$).

Cell lines derived from pseudoprogressing tumors increased the fraction of proliferating cells in response to the SG treatment

It is difficult to differentiate PP from real disease progression, when they initially emerge. Only, follow-up of enlarging lesions can distinguish PP from treatment failure.

In previous papers, we demonstrated that as a consequence of the SG treatment, there is an underlying repopulation (regrowth) mechanism that enhances the fraction of proliferating cells, and whose potency would be intrinsic to each tumor [24,25]. Owing to this regrowth effect before, during and after SG treatment, the long-term outcomes often differ from short-term cytotoxic effects. The PI defined as the cycling fraction of viable cells (in S, G_2/M and hyperdiploid phases), could help to predict these delayed reactions.

All canine cell lines (nine out of 17) derived from PP tumors (*Rka*, *Ay*, *Tr*, *Cl*, *Ov*, *Rk*, *Bk*, *Sc* and *Ds*), enhanced their basal proliferative phenotype in response to the SG treatment ($PI_{SG} > PI_B$; Fig. 2a and Table 1). This happened also in those cells derived from non-pseudoprogressing (NPP) tumors that displayed PR (*Bl* and *Ch*). Conversely, all NPP tumors displaying SD (*Rd*, *Br*, *Bt*, *Btl*, *Lo* and *Fk*) did not increase their basal proliferative state in response to SG treatment (PI_{SG} was similar to PI_B; Table 1). However, *Bk* and *Ds* (of 3 PP tumors that finally resolved in SD) increased their PI_{SG}.

Proliferation indexes correlated with the in-vivo and in-vitro tumor cells' response to suicide gene

The heterogeneous dynamic subpopulations of proliferating and growth-arrested melanomas cells leads to different tumor population growth rates before, during and after SG treatment. Then, the final SG outcome depends on the balance between PI_B-dependent 'regrowth resistance' versus 'regrowth sensitivity' to SG treatment (PI_{SG}).

As most conventional anticancer drugs, SG treatment was preferentially toxic for proliferating cells. As shown in Table 1, this 'regrowth sensitivity' to SG system depended on the proportion of cells capable of proliferating in response to this agent (PI_{SG}). Then, a reduced fraction of PI_{SG} could limit the effectiveness of cell cycle-dependent SG system.

As greater was the PI_{SG}, greater was the cell lines' response to SG in both spatial configurations, as confirmed by the high correlation ($P < 0.0001$) between both parameters (Fig. 3a). This in-vitro outcome reflected the in-vivo behavior. A significant correlation was found between the PI_{SG} and the in-vivo SG response of the respective tumors (Fig. 3b).

Fig. 3

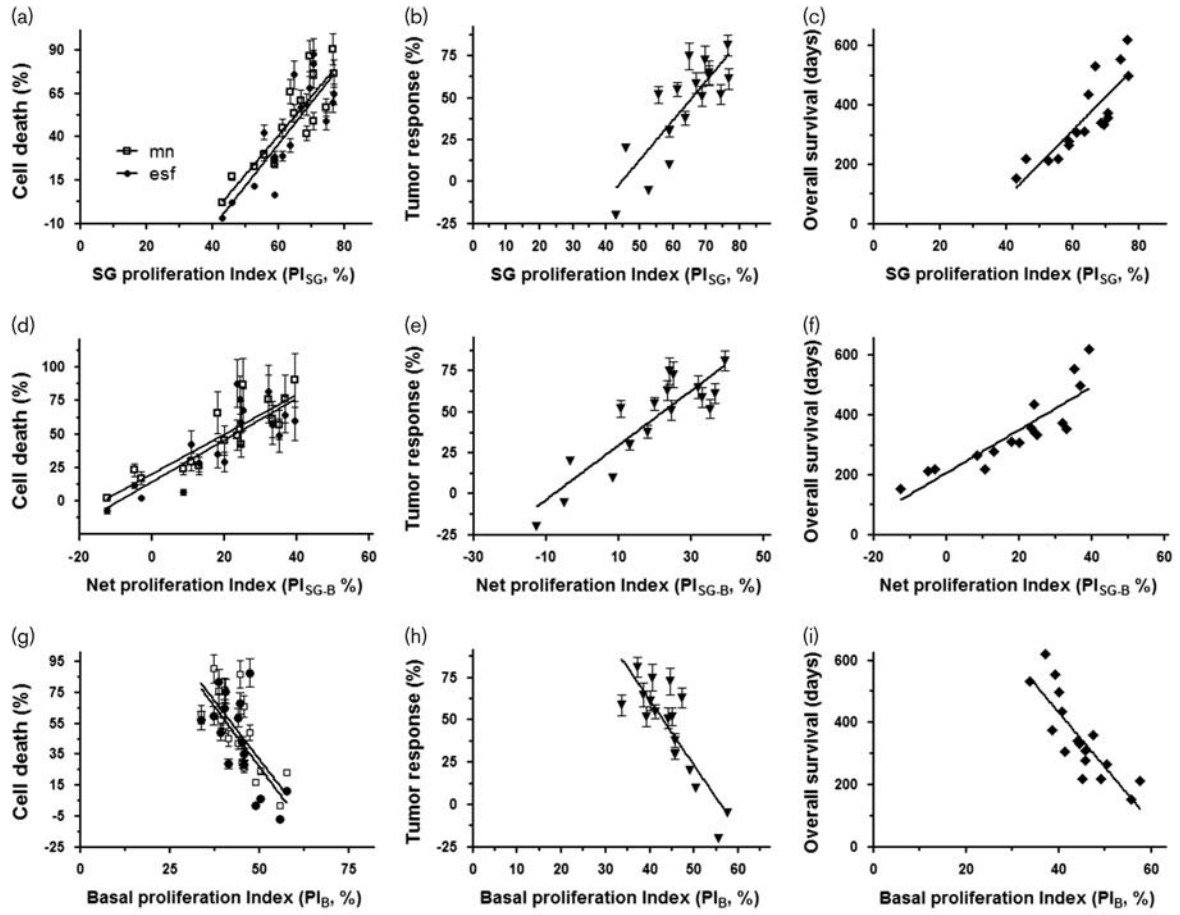

Proliferation Index	*In vivo* tumors		Spheroids		Monolayers		Survival	
	R^2	*P*<	R^2	*P*<	R^2	*P*<	R^2	*P*<
PI_{SG}	0.676	0.0001	0.694	0.0001	0.770	0.0001	0.723	0.0001
PI_{SG-B}	0.785	0.0001	0.679	0.0001	0.772	0.0001	0.810	0.0001
PI_B	0.714	0.0001	0.460	0.005	0.548	0.0005	0. 698	0.0001

Correlation between the suicide gene (SG) response of in-vivo tumors, spheroids, and monolayers, and the proliferation index of SG-treated cells (PI_{SG}, a, b), the net PI increase owing to SG treatment (PI_{SG-B}, c, d) and the basal proliferation index (PI_B) of control cells (PI_B, g, h). Statistical values were determined by the Pearson test with the GraphPad program.

All SG-sensitive cell lines significantly increased their PI_B in response to the SG treatment. Then, for each cell line, we calculated the net PI increase owing to SG treatment by subtracting the PI_B of the respective PI_{SG} (PI_{SG-B}) (Table 1). This net value allows the evaluation of the PI increase owing to the SG, independent of the basal replicative state (PI_B).

A remarkable finding was the strong correlation ($P < 0.0001$) between the net PI increase owing to SG (PI_{SG-B}) and the SG sensitivity of the in-vivo tumors (Fig. 3e) and of their derived cell lines in both spatial configurations (Fig. 3d).

In contrast, the basal proliferative state of melanoma cell lines (PI_B) exhibited an inverse correlation with the extent of their cell death to SG system in both spatial configurations (Fig. 3g). Accordingly, the response to SG of their respective in-vivo tumors also exhibited an inverse correlation with PI_B (Fig. 3h). Thus, as more aggressive was the tumor (greater PI_B of the cell line), more the balance displacement towards 'regrowth resistance' overcame SG cytotoxicity.

An interesting finding was that the overall survival of the veterinary patients to SG treatment also exhibited an inverse correlation with the PI_B (Fig. 3i) and a direct correlation with both PI_{SG} and PI_{SG-B} (Fig. 3c and f).

The growing capability of tumor-derived spheroids determined their sensitivity to suicide gene therapy

Unlike the exponential grow of monolayer cultures, cells growing as spheroids and solid tumors are characterized

by an increased polarization of melanoma cells toward enhanced dormancy, pluripotency, loss of differentiation, and invasiveness [26]. These heterogeneous cellular aggregates reproduce the 'regrowth repopulation' of the respective tumors through recruitment of the surviving quiescent cells to the proliferative fraction after SG

Fig. 4

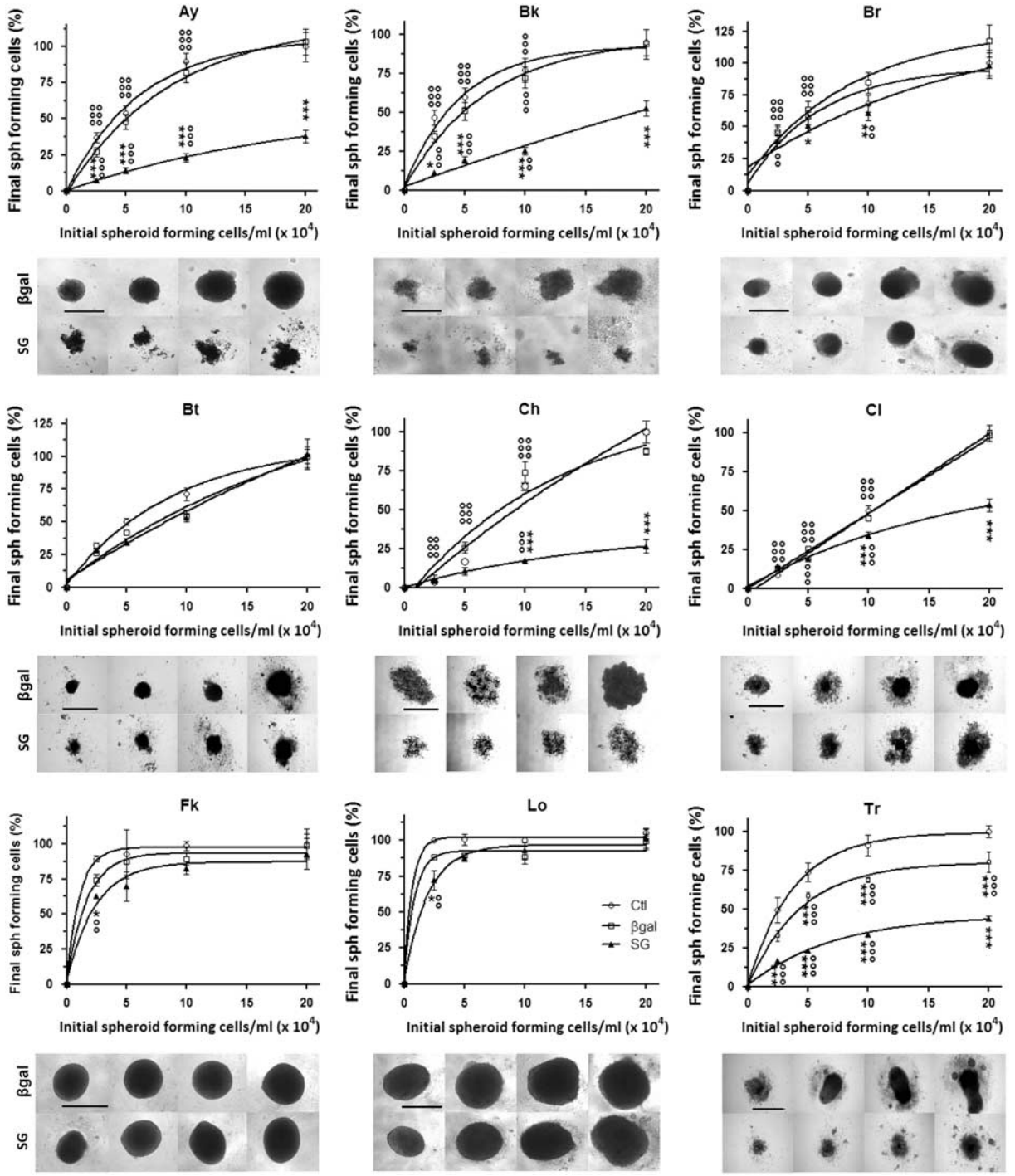

Effect of initial number of seeded control, *βgal*-expressing and SG-expressing cells on the growing capacity of tumor spheroids.*Versus its respective *βgal*; °versus its respective value of 20×10^4 cells/ml. Lower panels: Images represent final size and growth of individual spheroids formed by the number of cells described in the upper plots. Spheroids growing in suspension in 96-well plates for 13 days were photographed by inverted phase contrast microscope (×40). Bars: 500 μm.

treatment [25]. Thus, under conditions that more closely resemble the in-vivo situation, we explored how the growing capacity of tumor-derived spheroids could affect the efficacy of SG therapy.

As shown in the lower panels of Fig. 4, regardless of the initial number of seeded cells, all the tested lines formed unique spheroids. The patterns of growth, size, shape, and degree of compaction of the spheroids were characteristic of each cell line. *Ay*, *Br*, *Fk*, and *Lo* formed compact rounded spheroids with defined edges at all the evaluated cell concentrations. Conversely, *Bk*, *Bt*, *Ch*, *Cl*, and *Tr* cell lines generated loosely associated aggregates, in which single cells could be clearly distinguished. As control and *βgal*-expressing cells produced almost identical spheroids, only representative images of *βgal*-expressing spheroids were shown.

Depicting their proliferative status, both PP (*Ay*, *Bk*, *Cl* and *Tr)* and NPP tumors (*Br*, *Bt*, and *Ch*)-derived spheroids displayed an extensive growth during 13 days of culture ($P < 0.05$). In these lines, the final size of the spheroid increased according to the initial number of cells sown. These spheroids, that did not reach their maximum sizes, still maintained their growing ability. When treated with SG, these spheroids exhibited smaller size and a looser conformation than their respective control spheroid. *Ay*, *Bk*, *Ch*, *Cl*, and *Tr* spheroids were sensitive to SG system at all the evaluated cell densities ($P < 0.05$, Fig. 4).

Conversely, *Br* and *Bt* spheroids, derived from NPP tumors, exhibited low cytotoxicity to SG concurrently with a reduced $PI_{SG\text{-}B}$ (Fig. 4 and Table 1). This result suggests that, the fair lipofection efficiency (< 1%) of *Br* cell line reduced its SG sensitivity and then, its $PI_{SG\text{-}B}$. Conversely, a reduced fraction of cells capable of proliferating in response to SG (PI_{SG} similar to PI_B) in *Bt* spheroids could limit the effectiveness of cell cycle-dependent SG system.

In agreement with the highly aggressive phenotype of *Fk* and *Lo* tumors, their derived cell lines produced the biggest, dense, spherical, and regularly shaped spheroids.

Consistent with the faster in-vivo tumor growth, the spheroids of these lines reached the same size (their maximum size) regardless of the number of cells sown (Fig. 4). Only the spheroids formed with 2.5×10^4 cells/ml were sensitive to SG ($P < 0.05$) and decreased in size, without modifying their compact conformation. After reaching their definite size, *Fk* and *Lo* spheroids formed with larger number of cells, lost their SG sensitivity, simultaneously with their growing ability. Then, when the spheroid growth capacity is so high that it quickly reaches its plateau, regardless of the initial number of cells that gave rise to it (*Fk* and *Lo*), 'regrowth resistance' (PI_B) prevailed over 'regrowth sensitivity' to SG (PI_{SG}), limiting the effectiveness of this gene therapy approach.

Conclusion

In our veterinary clinical trials for canine melanoma that combine local and systemic immunotherapy, the repeated intratumor injections of SG, by killing cells in an 'immunogenic fashion', generates transitory increases of tumor size called PP [8–10,27]. The successful clinical outcome suggests that PP was part of a strong local antitumor response evidenced by a high proportion of objective responses and disease control, with a significant prolongation of median overall survival and disease free-survival [8–10].

The basis of this phenomenon that was also described for immunotherapy-treated human mucosal melanoma [28] is still not fully understood. Evidence of immune cells infiltrates, edema, and necrosis in the enlarged tumors supports the idea that PP may be owing to tumor inflammation [8,15,16,27]. However, broader evaluation across canine melanoma tumors and their derived cell lines suggests that increased vascular permeability and tumor regrowth owing to SG treatment also contributed to PP [8–10,27].

Despite inter-patient variability and the differences in tumor biology across disease sites, melanomas are composites of heterogeneous dynamic subpopulations of proliferating and growth-arrested cells [19–21]. This leads to different tumor population growth rates before, during, and after SG treatment, including accelerated repopulation during therapy. The PI, defined as the cycling fraction of viable cells (in S, G_2/M and hyperdiploid phases), is a dynamic factor that varied during the course of SG therapy. This parameter would reflect the in-vivo and in-vitro proportion of proliferating tumor cells in the absence of treatment (PI_B) or in response to SG (PI_{SG}). Their respective proportions during SG treatment could have a prognostic value for both in-vivo and in-vitro tumor cells' response to SG.

The data presented here suggest that the final SG outcome depends on the balance between PI_B-dependent 'regrowth resistance' versus 'regrowth sensitivity' to SG treatment (PI_{SG}). In those in-vivo and in-vitro tumor cells presenting PR to SG treatment, 'regrowth sensitivity' (PI_{SG}) prevailed over 'regrowth resistance' (PI_B). However, when the basal growth capacity of in-vivo and in-vitro melanoma cells (PI_B) was very high (*Fk* and *Lo*; Table 1 and Fig. 4), 'regrowth resistance' overcame 'regrowth sensitivity'.

Previous and present results suggest that the successful eradication of both PP and NPP tumors depends on the 'regrowth sensitivity' to SG treatment leading to an initial acceleration of tumor growth with proliferation and exhaustion of quiescent cells [8–10,24,25]. The high proportion of complete responses suggests that SG would strongly reduce the quiescent cells subpopulation by inducing its constant proliferation, repopulating activity, and differentiation, both *in vitro* and *in vivo* [8–10,24,25,29].

Furthermore, the direct correlation between PI_{SG} and the overall survival of our canine patients (Fig. 3c, f and i) recapitulate the data of our veterinary clinical trials where higher tumor responses correlated with longer overall survivals of our canine patients [8–10]. The analysis of serial biopsies taken throughout the treatment, as it was reported in some immunotherapeutic approaches [30] could have helped in a more detailed characterization of the PP process. Therefore, it will be included in further studies.

A better understanding of the evolution of individual patient's tumor characteristics such as PP, PI, 'regrowth sensitivity', and 'regrowth resistance' during the SG treatment could have a prognostic value for a personalized prediction of clinical efficacy and accurate management of melanoma patients.

Acknowledgements

The authors thank María D. Riveros and Graciela B. Zenobi for technical advice and assistance and all the VMDs involved in patients' treatment and care.

G.C.G. and L.M.E.F. are investigators, and C.F. and L.A. are fellows of the Consejo Nacional de Investigaciones Científicas y Técnicas (CONICET, Argentina).

This research was partially funded by grants from ANPCYT/FONCYT (PICT2012-1738 and PICT2014-1652) and CONICET (PIP 112 201101 00627 and PIP 11220150100885).

Conflicts of interest

There are no conflicts of interest.

References

1 Ramos-Vara JA, Beissenherz ME, Miller MA, Johnson GC, Pace LW, Fard A, *et al*. Retrospective study of 338 canine oral melanomas with clinical, histologic, and immunohistochemical review of 129 cases. *Vet Pathol* 2000; **37**:597–608.

2 Simpson RM, Bastian BC, Michael HT, Webster JD, Prasad ML, Conway CM, *et al*. Sporadic naturally occurring melanoma in dogs as a preclinical model for human melanoma. *Pigment Cell Melanoma Res* 2014; **27**:37–47.

3 Tarhini AA, Agarwala SS. Cutaneous melanoma: available therapy for metastatic disease. *Dermatol Ther* 2006; **19**:19–25.

4 Chin L, Garraway LA, Fisher DE. Malignant melanoma: genetics and therapeutics in the genomic era. *Genes Dev* 2006; **20**:2149–2182.

5 Smedley RC, Spangler WL, Esplin DG, Kitchell BE, Bergman PJ, Ho HY, *et al*. Prognostic markers for canine melanocytic neoplasms: a comparative review of the literature and goals for future investigation. *Vet Pathol* 2011; **48**:54–72.

6 Boston SE, Lu X, Culp WT, Montinaro V, Romanelli G, Dudley RM, *et al*. Efficacy of systemic adjuvant therapies administered to dogs after excision of oral malignant melanomas: 151 cases (2001–2012). *J Am Vet Med Assoc* 2014; **245**:401–407.

7 Tuohy JL, Selmic LE, Worley DR, Ehrhart NP, Withrow SJ. Outcome following curative-intent surgery for oral melanoma in dogs: 70 cases (1998–2011). *J Am Vet Med Assoc* 2014; **245**:1266–1273.

8 Finocchiaro LM, Fiszman GL, Karara AL, Glikin GC. Suicide gene and cytokines combined nonviral gene therapy for spontaneous canine melanoma. *Cancer Gene Ther* 2008; **15**:165–172.

9 Finocchiaro LM, Glikin GC. Cytokine-enhanced vaccine and suicide gene therapy as surgery adjuvant treatments for spontaneous canine melanoma. *Gene Ther* 2008; **15**:267–276.

10 Finocchiaro LM, Glikin GC. Cytokine-enhanced vaccine and suicide gene therapy as surgery adjuvant treatments for spontaneous canine melanoma: 9 years of follow-up. *Cancer Gene Ther* 2012; **19**:852–861.

11 Finocchiaro LM, Fondello C, Gil-Cardeza ML, Rossi Ú, Villaverde MS, Riveros MD, *et al*. Cytokine-enhanced vaccine and interferon-β plus suicide gene therapy as surgery adjuvant treatments for spontaneous canine melanoma. *Hum Gene Ther* 2015; **26**:367–376.

12 Hodi FS, O'Day SJ, McDermott DF, Weber RW, Sosman JA, Haanen JB, *et al*. Improved survival with ipilimumab in patients with metastatic melanoma. *N Engl J Med* 2010; **363**:711–723.

13 Hodi FS, Hwu WJ, Kefford R, Weber JS, Daud A, Hamid O, *et al*. Evaluation of immune-related response criteria and RECIST v1.1 in patients with advanced melanoma treated with pembrolizumab. *J Clin Oncol* 2016; **34**:1510–1517.

14 Constantino J, Gomes C, Falcão A, Neves BM, Cruz MT. Dendritic cell-based immunotherapy: a basic review and recent advances. *Immunol Res* 2017; **65**:798–810.

15 Chiou VL, Burotto M. Pseudoprogression and immune-related response in solid tumors. *J Clin Oncol* 2015; **33**:3541–3543.

16 Chae YK, Wang S, Nimeiri H, Kalyan A, Giles FJ. Pseudoprogression in microsatellite instability-high colorectal cancer during treatment with combination T cell mediated immunotherapy: a case report and literature review. *Oncotarget* 2017; **8**:57889–57897.

17 Glikin GC, Finocchiaro LM. Clinical trials of immunogene therapy for spontaneous tumors in companion animals. *ScientificWorldJournal* 2014; **2014**:718520.

18 Finocchiaro LME, Glikin GC. Recent clinical trials of cancer immunogene therapy in companion animals. *World J Exp Med* 2017; **7**:42–48.

19 Quintana E, Shackleton M, Foster HR, Fullen DR, Sabel MS, Johnson TM, *et al*. Phenotypic heterogeneity among tumorigenic melanoma cells from patients that is reversible and not hierarchically organized. *Cancer Cell* 2010; **18**:510–523.

20 Somasundaram R, Villanueva J, Herlyn M. Intratumoral heterogeneity as a therapy resistance mechanism: role of melanoma subpopulations. *Adv Pharmacol* 2012; **65**:335–359.

21 Hendrix MJ, Seftor EA, Hess AR, Seftor RE. Molecular plasticity of human melanoma cells. *Oncogene* 2003; **22**:3070–3075.

22 Hendrix MJ, Seftor EA, Chu YW, Seftor RE, Nagle RB, McDaniel KM, *et al*. Coexpression of vimentin and keratins by human melanoma tumor cells: correlation with invasive and metastatic potential. *J Natl Cancer Inst* 1992; **84**:165–174.

23 Zhao WY, Xu J, Wang M, Zhang ZZ, Tu L, Wang CJ, *et al*. Prognostic value of Ki67 index in gastrointestinal stromal tumors. *Int J Clin Exp Pathol* 2014; **7**:2298–2304.

24 Agnetti L, Fondello C, Villaverde MS, Glikin GC, Finocchiaro LME. Therapeutic potential of bleomycin plus suicide or interferon-β gene transfer combination for spontaneous feline and canine melanoma. *Oncoscience* 2017; **4**:199–214.

25 Gil-Cardeza ML, Villaverde MS, Fiszman GL, Altamirano NA, Cwirenbaum RA, Glikin GC, *et al*. Suicide gene therapy on spontaneous canine melanoma: correlations between in vivo tumors and their derived multicell spheroids in vitro. *Gene Ther* 2010; **17**:26–36.

26 Sutherland RM. Cell and environment interactions in tumor microregions: the multicell spheroid model. *Science* 1988; **240**:177–184.

27 Villaverde MS, Combe K, Duchene AG, Wei MX, Glikin GC, Finocchiaro LM. Suicide plus immune gene therapy prevents post-surgical local relapse and increases overall survival in an aggressive mouse melanoma setting. *Int Immunopharmacol* 2014; **22**:167–175.

28 Atrash S, Makhoul I, Mizell JS, Hutchins L, Mahmoud F. Response of metastatic mucosal melanoma to immunotherapy: it can get worse before it gets better. *J Oncol Pharm Pract* 2017; **23**:215–219.

29 Fondello C, Agnetti L, Villaverde MS, Simian M, Glikin GC, Finocchiaro LME. The combination of bleomycin with suicide or interferon-β gene transfer is able to efficiently eliminate human melanoma tumor initiating cells. *Biomed Pharmacother* 2016; **83**:290–301.

30 Paoloni M, Mazcko C, Selting K, Lana S, Barber L, Phillips J, *et al*. Defining the pharmacodynamic profile and therapeutic index of NHS-IL12 immunocytokine in dogs with malignant melanoma. *PLoS ONE* 2015; **10**:e0129954.